JOURNAL OF VIROLOGY, Apr. 2005, p. 4764–4773 Vol. 79, No. 8
0022-538X/05/$08.00+0 doi:10.1128/JVI.79.8.4764–4773.2005

Expression of Matrix Metalloproteinases and Their Tissue Inhibitor during Viral Encephalitis

Jiehao Zhou,[1] Norman W. Marten,[1] Cornelia C. Bergmann,[1,2] Wendy B. Macklin,[3] David R. Hinton,[1] and Stephen A. Stohlman[1,2,4]*

Departments of Pathology,[1] Neurology,[2] and Molecular Microbiology and Immunology,[4] Keck School of Medicine, University of Southern California, Los Angeles, California, and Department of Neurosciences, The Cleveland Clinic Foundation, Cleveland, Ohio[3]

Received 27 August 2004/Accepted 1 December 2004

Matrix metalloproteinases (MMPs) participate in remodeling the extracellular matrix and facilitate entry of inflammatory cells into tissues. Infection of the murine central nervous system (CNS) with a neurotropic coronavirus induces encephalitis associated with increased levels of mRNA encoding MMP-3 and MMP-12. Whereas virus-induced MMP-3 expression was restricted to CNS resident astrocytes, MMP-12 mRNA was expressed by both inflammatory cells and CNS resident cells. Immunosuppression increased both MMP-3 and MMP-12 mRNA levels in CNS resident cells, suggesting that the presence of virus rather than inflammation induced protease up-regulation. MMP activity is partially regulated by a small family of genes encoding tissue inhibitors of matrix metalloproteinases (TIMPs); among the TIMPs, only TIMP-1 mRNA expression increased in the CNS following coronavirus infection. During inflammation TIMP-1 mRNA was most prominently expressed by infiltrating cells. By contrast, in the immunosuppressed host TIMP-1 mRNA was expressed by CNS resident cells. Analysis of cytokine and chemokine mRNA induction within the infected CNS of healthy and immunocompromised mice suggested a possible correlation between increased viral replication and increased levels of beta interferon, MMP-3, MMP-12, and TIMP-1 mRNA. CD4$^+$ T cells which localize to the perivascular and subarachnoid spaces were identified as the primary source of TIMP-1 protein. By contrast, protein expression was undetectable in astrocytes or CD8$^+$ T cells, the primary antiviral effectors that localize to the CNS parenchyma in response to infection. These data suggest that in contrast to the results seen with MMPs, inhibition of protease activity via TIMP-1 expression correlates with the differential tissue distribution of T-cell subsets during acute coronavirus-induced encephalitis.

Recruitment of mononuclear cells into sites of inflammation involves a number of distinct steps that include tethering to endothelia, rolling, integrin activation, and extravasation into the perivascular space (25). Lymphocyte trafficking into the central nervous system (CNS), induced by either infection or autoimmunity, is limited by several additional impediments. These include both the cellular and extracellular matrix (ECM) components of the blood brain barrier (BBB) as well as limited parenchymal extracellular spaces (25, 32). During CNS inflammation, matrix metalloproteinases (MMPs) degrade the basal laminal components of capillaries and contribute to BBB disruption (23, 25, 32), thereby facilitating lymphocyte trafficking. MMPs belong to a large family of endoproteinases associated with ECM remodeling during development, morphogenesis, angiogenesis, pregnancy, and wound healing in addition to affecting inflammatory responses (18, 29, 32). MMPs not only participate in normal physiological processes and inflammation but are also associated with tumor metastasis, arthritis, tissue ulcers, and neurological diseases, e.g., Alzheimer's disease and multiple sclerosis (MS) and its animal model, experimental autoimmune encephalomyelitis (EAE) (11, 20, 32). The CNS responds to inflammatory events by increasing mRNA encoding a variety of MMPs and tissue inhibitors of MMPs (TIMPs). For example, CD4$^+$ T-cell-mediated EAE induces MMP-3, -7, -8, -9, -10, -12, -13, and -14 and TIMP-1 within the CNS (19, 21). Increased MMP expression and/or decreased expression of TIMPs is associated with increased MS clinical activity (11, 20, 31, 32). These data are consistent with the ability of MMP inhibitors to prevent EAE (4) and imply a distinct proinflammatory role for MMPs in the pathogenesis of CD4$^+$ T-cell-mediated autoimmune CNS disease.

CD8$^+$ T cells are the primary effectors of virus control during coronavirus-induced encephalitis (17). They enter the CNS parenchyma and suppress viral replication via a combination of perforin-mediated cytolysis and gamma interferon (IFN-γ) secretion (17, 27). Although cellular components of both innate and adaptive arms of the immune system are recruited into the CNS during coronavirus-induced acute encephalitis, only a limited number of the broad potential spectrum of MMP mRNAs are induced (33). MMP-9 mRNA levels are not increased; however, the ability of inflammatory cells to extravasate through blood vessels and traverse the BBB during coronavirus-induced encephalitis correlates with increased levels of preformed MMP-9 protein derived from neutrophils (34). Only MMP-3, MMP-12, and TIMP-1 mRNA expression increases within the CNS in response to acute coronavirus encephalitis (33). To reach parenchymal sites of viral infection, CD8$^+$ T cells must overcome both the physical barrier represented by the BBB as well as the CNS parenchymal ECM (2, 12, 23, 25, 32). By contrast, CD4$^+$ T cells, vital for parenchymal CD8$^+$ T-cell survival, are retained within the subarachnoid

* Corresponding author. Mailing address: 1333 San Pablo St., MCH 142, Los Angeles, CA 90033. Phone: (323) 442-1036. Fax: (323) 225-2369. E-mail: stohlman@usc.edu.

TABLE 1. Real-time PCR primer sequences

Gene	5′ primer	3′ primer
Ubiquitin	TGGCTATTAATTATTCGGTCTGCAT	GCAAGTGGCTAGAGTGCAGAGTAA
MMP-2	TTCCCTAAGCTCATCGCAGACT	CACGCTCTTGAGACTTTGGTTCT
MMP-3	TTTAAAGGAAATCAGTTCTGGGCTATA	CGATCTTCTTCACGGTTGCA
MMP-9	CCATGCACTGGGCTTAGATCAT	CAGATACTGGATGCCGTCTATGTC
MMP-12	GGAGCTCACGGAGACTTCAACT	CCTTGAATACCAGGTCCAGGATA
MMP-14	TAAGCACTGGGTGTTTGACGAA	CCCTCGGCCAAGCTCCT
TIMP-1	CCAGAGCCGTCACTTTGCTT	AGGAAAAGTAGACAGTGTTCAGGCTT
TIMP-2	ACGCTTAGCATCACCCAGAAG	TGGGACAGCGAGTGATCTTG
TIMP-3	ATCCCCAGGATGCCTTCTG	CCCTCCTTCACCAGCTTCTTT
IL-1α	TGGTGTGTGACGTTCCCATT	CCGACAGCACGAGGCTTT
IL-1β	GACGGCACACCCACCCT	AAACCGTTTTTCCATCTTCTTCTTT
IL-6	ACACATGTTCTCTGGGAAATCGT	AAGTGCATCATCGTTGTTCATACA
IFN-β	GCTCCTGGAGCAGCTGAATG	CGTCATCTCCATAGGGATCTTGA
IFN-γ	TGATGGCCTGATTGTCTTTCAA	GGATATCTGGAGGAACTGGCAA
TNF-α	GCCACCACGCTCTTCTGTCT	GGTCTGGGCCATAGAACTGATG
CCL-2	GCTGGAGCATCCACGTGTT	ATCTTGCTGGTGAATGAGTAGCA
CCL-5	GCAAGTGCTCCAATCTTGCA	CTTCTCTGGGTTGGCACACA

spaces and perivascular areas (17, 27). The potential role(s) of MMP-3, MMP-12, and TIMP-1 in regulating the differential $CD8^+$ and $CD4^+$ T-cell migration into the CNS parenchyma during acute virus-induced encephalitis was examined by analysis of mRNA derived from both CNS resident and inflammatory cells and by immunohistochemistry. Astrocytes were the prominent source of MMP-3 in both infected immunocompetent and infected immunosuppressed mice. By contrast, MMP-12 was expressed by multiple CNS resident and infiltrating cell types. However, similar to MMP-3, MMP-12 expression in resident cells was enhanced in immunosuppressed mice. Enhanced MMP expression in the CNS of immunosuppressed mice correlated with increased viral replication, increased IFN-β mRNA levels, and increased TIMP-1 mRNA induction in CNS resident cells, suggesting virus-induced MMP activation. However, in the presence of an inflammatory response TIMP-1 protein expression was undetectable in astrocytes, microglia-macrophages, or $CD8^+$ T-cell effectors, which localized to the areas of parenchymal infection. By contrast, TIMP-1 protein was almost exclusively expressed by $CD4^+$ T cells localized to the perivascular and subarachnoid spaces. The differential expression of TIMP-1 by perivascular $CD4^+$ T cells, and its absence from parenchymal $CD8^+$ T cells, suggests a novel role for TIMP-1 in regulating differential T-cell recruitment into the CNS parenchyma during coronavirus-induced encephalitis.

MATERIALS AND METHODS

Mice and viruses. C57BL/6 male mice were purchased from the National Cancer Institute (Frederick, Md.). Mice between 6 and 8 weeks of age were infected intracerebrally with 250 PFU of the 2.2-V-1 variant of the neurotropic JHM strain of mouse hepatitis virus (JHMV) (7) in a volume of 30 μl of sterile endotoxin-free phosphate-buffered saline (PBS). For immunosuppression, mice were irradiated with 9.5 Gy from a ^{137}Cs gamma vertical beam source 24 h prior to infection (22, 23). CNS virus titers were determined by plaque assay of clarified brain homogenates adsorbed onto monolayers of DBT cells as previously described (7). All procedures were performed in compliance with Keck School of Medicine Institutional Animal Care and Use Committee-approved protocols.

Isolation of CNS-derived cells. Cells were isolated from the CNS of mice perfused via intracardiac injection of 50 ml of PBS. For CNS inflammatory cells, including neutrophils, macrophages, NK cells, microglia, and T cells, brains were homogenized in RPMI medium supplemented with 25 mM HEPES (pH 7.2) and 1% fetal bovine serum by the use of ice-cold Tenbroeck tissue homogenizers. For CNS resident cells, including an astrocyte-enriched population and oligodendroglia, tissues were minced at 4°C and digested with trypsin (0.25% final concentration) for 30 min at 37°C with agitation. Digestion was terminated by addition of an equal volume of ice-cold RPMI medium containing 20% fetal calf serum. For both types of preparations, cells were suspended in 30% Percoll (Pharmacia, Piscataway, N.J.) and concentrated onto 1 ml of 70% Percoll by centrifugation at $800 \times g$ for 20 min at 4°C (3, 34). Cells were collected from the 30%Percoll–70% Percoll interface and washed twice with RPMI medium prior to analysis.

Prior to flow cytometry, nonspecific binding was minimized by incubation with purified rat anti-mouse FcIII/IIR monoclonal antibody (MAb) (2.4G2; BD PharMingen, San Diego, Calif.) diluted in PBS containing 2% mouse serum and 0.5% bovine serum albumin (Sigma Chemical Company, Saint Louis, Mo.) for 15 min at 4°C. Surface expression was determined with MAb specific for CD8 (53-6.7), CD4 (GK1.5), NK1.1 (PK136), Ly-6G and Ly-6C (RB6-8C5), major histocompatibility complex class II (2G9), CD45 (30-F11), CD11b (M1/70) (all from BD PharMingen), and F4/80 (Cl:A3-1) (Serotech, Raleigh, N.C.). Oligodendroglia were identified using MAb O4 as previously described (9). Cells were stained for 30 min on ice and isolated using a FACSDiVa flow cytometer (Becton Dickinson, Mountain View, Calif.). Populations identified were $CD4^+$ T cells ($CD45^{hi}CD4^+$), $CD8^+$ T cells ($CD45^{hi}CD8^+$), NK cells ($CD45^{hi}NK1.1^+$), neutrophils ($CD45^{hi}Ly6G^{hi}CD11b^+$), macrophages ($CD45^{hi}F4/80^+$major histocompatibility complex class II^+), microglia ($CD45^{low}$), oligodendroglia ($CD45^-O4^+$), and an astrocyte-enriched population ($CD45^-O4^-$). Approximately 60% of the astrocyte-enriched population expressed glial fibrillary acidic protein (GFAP) as determined by staining with anti-GFAP MAb (Dako, Carpenteria, Calif.).

Gene expression analysis. RNA was prepared from the brains of individual mice ($n = 3$ to 5/group) by homogenization in guanidine isothiocyanate and isolated by centrifugation through 5.7 M cesium chloride as previously described (22). RNA from cell populations isolated from the CNS by fluorescence-activated cell sorting (FACS) was prepared from four to seven pooled mice per group by the use of Trizol reagent (GIBCO BRL, Rockville, Md.). Splenic $CD4^+$ T cells were prepared by positive selection using anti-L3T4-coated magnetic beads (Miltenyi Biotech Inc., Auburn, Calif.). Purity was assessed by flow cytometry using fluorescein isothiocyanate (FITC)-labeled anti-CD4, phycoerythrin-labeled anti-$CD8^+$, and FITC-labeled anti-CD19 (BD PharMingen). $CD4^+$ T cells were enriched to >96%. Purified $CD4^+$ T cells were activated by incubation for 12 h in RPMI medium containing 10% fetal calf serum, 500 ng of phorbol myristate acetate (PMA)/ml, and 1 μM ionomycin. RNA from untreated and activated $CD4^+$ T-cell populations was prepared using Trizol reagent (GIBCO BRL). DNA was eliminated with a DNA-Free kit (Ambion, Austin, Tex.). Reverse transcription used AMV reverse transcriptase (Promega, Madison, Wis.) (22). Semiquantitative RNA expression used an ABI 5700 SDS PCR thermocycler (Applied Biosystems, Foster City, Calif.) and SYBR green reagents. Primer pairs used for analysis are described in Table 1. Amplification linearity of each primer pair was confirmed to have a correlation coefficient of >0.98 by measuring fivefold dilutions of cDNA samples. Cycle threshold (C_t) values are defined as the cycle number at which fluorescence exceeded a thresh-

old value of 0.5. Levels were normalized relative to ubiquitin mRNA and converted to a linearized value using the following formula: $1.8^{(Ct_{\text{ubiquitin}} - Ct_{\text{gene x}})} \times 10^5$.

Histopathology. Frozen sections (6 μm) were fixed in acetone for 15 min at room temperature and incubated with goat anti-human MMP-3 antibody, goat anti-mouse MMP-12 antibody, rabbit anti-human TIMP-1 antibody (Santa Cruz Biotechnology, Santa Cruz, Calif.), anti-CD4 MAb (L3T4), or anti-CD8 MAb (53-6.7) (BD PharMingen). Biotinylated secondary Ab (Vector Laboratory, Burlingame, Calif.) complexes were visualized using avidin-biotin peroxidase and NovaRED substrate (Vectastain-ABC kit; Vector Laboratory). Slides were read in a blinded fashion. For confocal microscopy, sections were fixed in 4% paraformaldehyde for 15 min at room temperature. Coexpression of MMP-3 and GFAP was detected with goat anti-human MMP-3 antibody (Santa Cruz Biotechnology), FITC-conjugated donkey anti-goat antibody (Chemicon, Temecula, Calif.), mouse anti-human GFAP MAb (Dako Corporation), and tetramethyl rhodamine isothiocyanate-conjugated rabbit anti-mouse antibody (Chemicon). Coexpression of TIMP-1 and CD4 employed rabbit anti-human TIMP-1 antibody (Santa Cruz Biotechnology), Cy3-conjugated goat anti-rabbit antibody (Chemicon), rat anti-mouse CD4 antibody (BD PharMingen), and FITC-conjugated rabbit anti-rat antibody (Chemicon). Slides were examined using a Zeiss LSM510 confocal microscope.

$CD4^+$ T-cell purification. Splenocytes were depleted of B cells by adsorption onto 150-mm-diameter plates coated with goat anti-mouse immunoglobulin (ICN Pharmaceuticals, Costa Mesa, Calif.). Following B-cell depletion, $CD4^+$ T cells were purified by positive selection using anti-CD4 (MAb GK1.5)-coated magnetic beads (Miltenyi Biotec Inc.). Purity was assessed by flow cytometry using phycoerythrin-labeled anti-$CD8^+$ antibody (clone 53-6.7), FITC-labeled anti-CD4 MAb (clone GK1.5), and FITC-labeled anti-CD19 MAb (clone 1D3) (BD PharMingen). $CD4^+$ T cells were enriched to >98%. $CD4^+$ T cells were activated by incubation in the presence of 500 ng of PMA/ml and 1 μM ionomycin for 12 h at 37 C. RNA was extracted as described above, and the mRNA expression levels determined by real-time PCR was compared to the results seen with untreated $CD4^+$ T cells relative to the housekeeping ubiquitin mRNA expression.

Statistical analysis. Results from three or more samples per experiment are represented as means ± standard deviations (SD) as analyzed using the Student's *t* test. Results from duplicate experiments are presented as means ± ranges.

RESULTS

Distinct patterns of MMP and TIMP expression by CNS inflammatory and resident cells. RNase protection assays of the murine CNS infected with a neurotropic coronavirus suggested an early increase in MMP-3, MMP-12, and TIMP-1 mRNA expression (33). Expression levels peaked coincident with maximal viral replication at day 6 postinfection (p.i.) but prior to maximum inflammation (33). Both the limited expression of MMP-3, MMP-12, and TIMP1 and the quantitation of mRNA levels were confirmed by real-time PCR (Fig. 1A). In the naïve CNS MMP-3 was undetectable, whereas MMP-12 and TIMP-1 mRNA were detected at low levels (Fig. 1A), consistent with previous data (11, 19, 20, 21, 32). During immunity-mediated virus clearance from the CNS the expression of MMP-3 and MMP-12 mRNA diminished precipitously by day 8 p.i. By contrast, TIMP-1 mRNA remained elevated over basal levels to day 14 p.i., the last time point examined (Fig. 1A). Previous studies revealed no alterations in MMP-1, MMP-2, MMP-7, MMP-9, MMP-10, MMP-11, MMP-13, MMP-14, TIMP-2, or TIMP-3 mRNA levels in the CNS during coronavirus-induced encephalitis as determined by an RNase protection assay (33). These findings were confirmed by results showing minimal (<2-fold) changes in the mRNA encoding MMP-2, MMP-9, MMP-14, TIMP-2, and TIMP-3 as detected by real-time PCR analysis over the course of CNS infection (data not shown). Restricted induction of MMPs and TIMPs by virus infection thus contrasts with the increased expression of numerous MMPs and TIMPs associated with autoimmune inflammation in both the human and the rodent CNS (11, 19, 20, 21, 22, 30).

To distinguish the expression levels of MMP-3, MMP-12, and TIMP-1 mRNA in infiltrates and CNS resident cells, single-cell suspensions from the CNS were separated into a $CD45^-$ population, comprising resident cells including astrocytes and oligodendroglia, $CD45^{low}$ microglia (8), and $CD45^{hi}$ bone marrow-derived infiltrating leukocytes as depicted in Fig. 1B. At day 6 p.i., MMP-3 mRNA was mainly expressed by $CD45^-$ CNS resident cells (Fig. 1C), although minimal expression was also detected in $CD45^{low}$ microglia and $CD45^{hi}$ infiltrating cells. By contrast, MMP-12 mRNA was expressed by infiltrating cells, microglia, and CNS resident cells (Fig. 1C). TIMP-1 mRNA expression was most abundant in the CNS-infiltrating population. Nevertheless, TIMP-1 mRNA levels were also increased in CNS resident cell populations during infection, with higher levels in $CD45^-$ compared to those seen with $CD45^{low}$ microglia (Fig. 1C). These data demonstrate differential expression of protease mRNA by CNS resident and inflammatory cells. Prominent TIMP-1 expression by infiltrating cells distinguishes virus-induced encephalitis from EAE in which TIMP-1 expression is confined to resident astrocytes (19, 21).

Immunosuppression increases MMP and TIMP mRNA expression. The contribution of inflammation to expression of MMP-3, MMP-12, and TIMP-1 mRNA in the CNS was examined by comparing immunocompetent with immunosuppressed mice at day 6 p.i. Immunosuppression eliminated the $CD45^{hi}$ inflammatory cells, resulting in a flow cytometric pattern identical to that seen with naïve mice (Fig. 2A). Furthermore, expression of neutrophil- and macrophage-specific mRNA (elastase and myeloperoxidase) decreased to undetectable levels in the CNS of the immunosuppressed mice, in contrast to the results seen with untreated mice (data not shown). Consistent with the uncontrolled virus replication in the absence of adaptive immunity (Fig. 2B) (3, 22, 33), levels of mRNA encoding the viral nucleocapsid protein increased approximately sevenfold in the CNS of infected immunosuppressed compared to immunocompetent mice at day 6 p.i. (data not shown). Immunosuppression further increased MMP-3, MMP-12, and TIMP-1 mRNA expression compared to the levels expressed in the CNS of immunocompetent mice (Fig. 3). Similar to the results seen with the CNS of infected immunocompetent mice, expression levels of mRNAs encoding other MMPs (MMP-2, MMP-9, and MMP-14) or TIMPs (TIMP-2 and TIMP-3) were not significantly altered in the CNS of infected immunocompromised mice (33; data not shown). In immunosuppressed mice, MMP-3 mRNA expression was confined to $CD45^-$ resident cells, whereas MMP-12 mRNA was expressed by both CNS resident $CD45^-$ cells and $CD45^{low}$ microglia (Fig. 3). Therefore, the ubiquitous MMP-12 mRNA expression and more restricted expression of MMP-3 mRNA were independent of inflammation (Fig. 3). Immunosuppression resulted in a further increase in TIMP-1 mRNA expression, albeit only within the $CD45^-$ CNS cells (Fig. 3). Thus, increased expression of TIMP-1 by CNS resident cells may represent a physiological attempt to compensate for potentially destructive effects of enhanced MMP-3 and MMP-12 expression. These data suggest that virus replication directly triggers up-regulation of

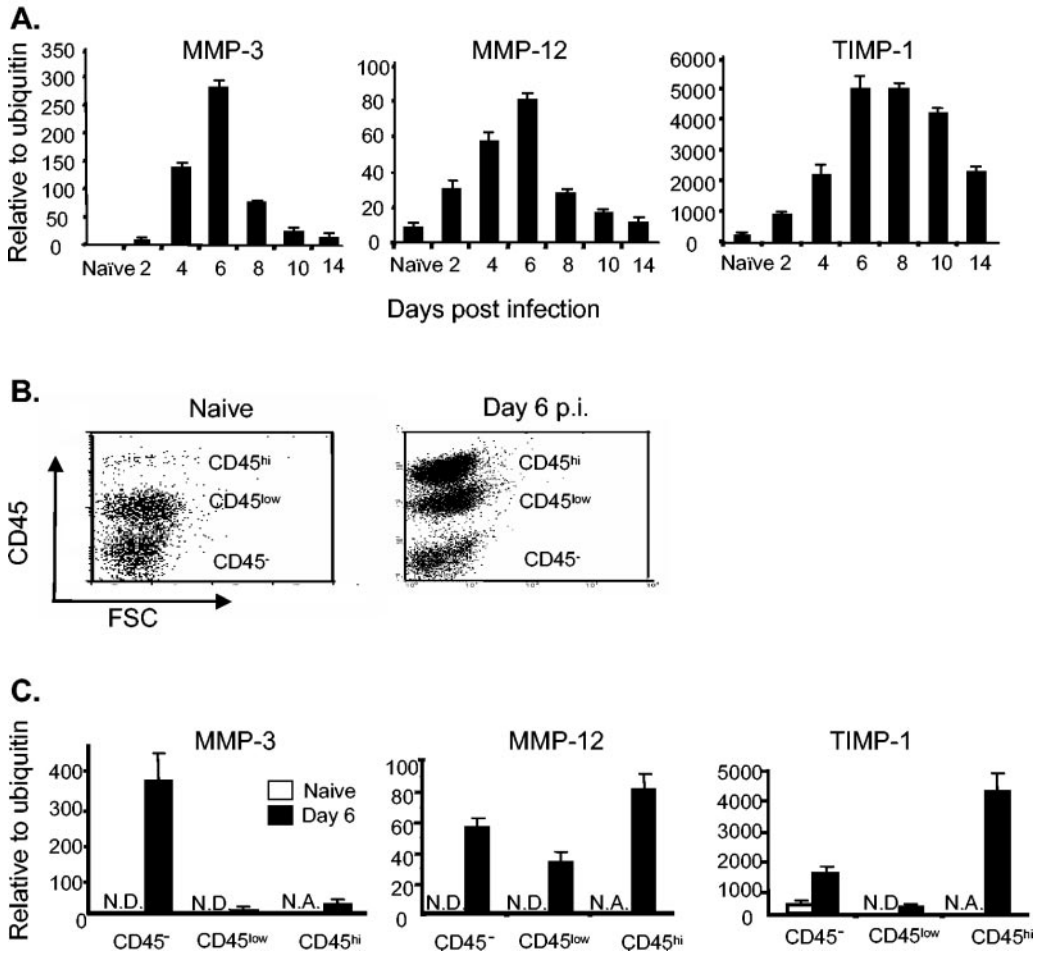

FIG. 1. Selective up-regulation of MMP-3, MMP-12, and TIMP-1 mRNA during viral encephalitis. (A) MMP-3, MMP-12, and TIMP-1 mRNA expression in brains of naïve and infected mice determined by semiquantitative real-time PCR. Data representing the average ± SD for three to five mice per group are presented in units relative to ubiquitin mRNA expression levels. (B) Flow cytometric analysis of CD45-expressing brain cells isolated from naïve or infected mice at day 6 p.i. (C) Comparison of MMP-3, MMP-12, and TIMP-1 mRNA expression in the $CD45^{-}$ CNS resident cells, $CD45^{low}$ microglia, and $CD45^{hi}$ bone-marrow-derived cells from infected mice at day 6 p.i. Data represent the average results of three separate experiments. Error bars represent SD. N.D., not detectable. N.A., not applicable.

MMP-3, MMP-12, and TIMP-1 mRNA expression. However, it is not clear whether the reduced mRNA expression detected in the immunocompetent hosts reflects reduced virus replication, inflammation, or a combination of both factors.

A variety of factors, including cytokines and chemokines, associated with encephalitogenic responses induce increased expression of MMP and TIMP mRNAs and proteins (11, 18, 29, 32). Expression of several mRNAs encoding cytokines and chemokines known to affect MMP and TIMP expression (5, 11, 16, 18, 29, 32) increased in the CNS during infection (Table 2), consistent with previous data (10, 22, 26). Expression of the mRNA encoding tumor necrosis factor alpha (TNF-α) peaked at day 4 p.i., while that of other cytokines associated with innate immunity (interleukin-1 alpha [IL-1α], IL-1β, IL-6, and IFN-β) peaked at day 6 p.i. Expression of IFN-γ mRNA and the mRNA encoding the chemokines CCL2 and CCL5 peaked at day 8 p.i., consistent with the maximal influx of CNS inflammatory cells (17, 33). The mRNA kinetics suggested an association between the induction of MMP-3, MMP-12, and TIMP-1 with cytokines associated with innate immunity. Potential mediators of virus-induced expression of MMP and TIMP mRNA were thus further examined by comparing mRNA from the CNS of infected immunocompetent and immunosuppressed mice. Immunosuppression did not alter IL-6 or TNF-α mRNA levels in the infected CNS (Fig. 4). By contrast, mRNA levels of IL-1α and IL-1β, the other innate cytokines, decreased substantially. The most dramatic change was noted in the ~10-fold up-regulation of IFN-β mRNA expression in the CNS of infected immunosuppressed mice (Fig. 4). As expected, IFN-γ, CCL2, and CCL5 mRNA expression decreased in the absence of inflammation (Fig. 4). Increased expression of MMP-3, MMP-12, and TIMP-1 mRNA in the CNS of infected immunosuppressed mice was thus associated with a dramatic increase in levels of IFN-β and decrease in levels of IL-1α and IL-1β. Although the possibility that IL-1α and IL-1β negatively regulate MMP and TIMP expression cannot be ruled out, these data are consistent with the concept that virus-induced IFN-β secretion by CNS resident cells may direct expression of the limited number of potential proteases as well as a single specific MMP inhibitor.

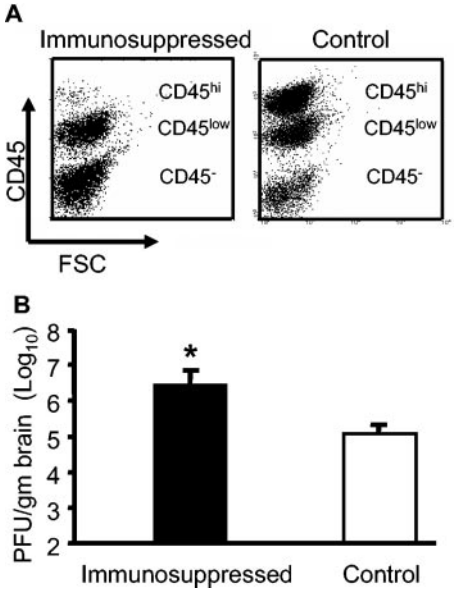

FIG. 2. Absence of inflammatory cells and increased infectious virus following immunosuppression. (A) Flow cytometric analysis of CNS-derived cells prepared from JHMV-infected immunosuppressed mice and wild-type controls at day 6 p.i. (A) Note the absence of $CD45^{hi}$ bone-marrow-derived inflammatory cells and retention of $CD45^{low}$ microglia. (B) Increased infectious virus levels in the CNS of immunosuppressed versus untreated infected mice. Data represent the average of duplicate determinations for a minimum of three mice in each group.

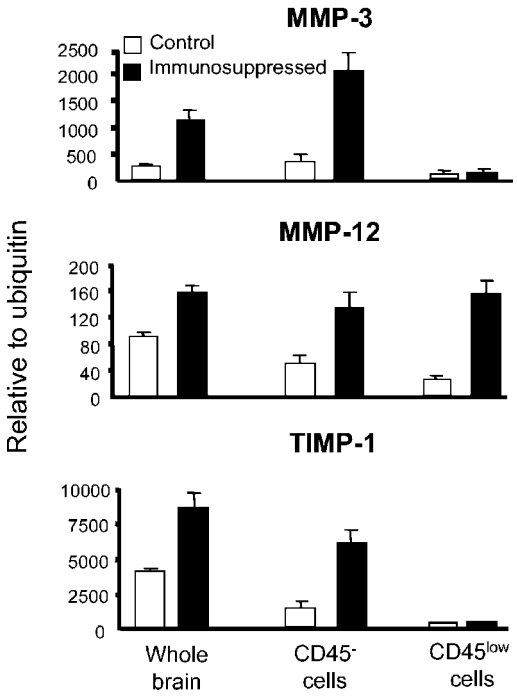

FIG. 3. Enhanced MMP-3, MMP-12, and TIMP-1 mRNA expression in the CNS of immunosuppressed hosts following infection. The results of a comparison of the levels of MMP-3, MMP-12, and TIMP-1 mRNA expression in unfractionated brain, $CD45^-$ CNS resident cells, and $CD45^{low}$ microglia derived from untreated infected and immunosuppressed infected mice at day 6 p.i. are shown. Data represent average results of two separate experiments. Error bars represent ranges of experimental results.

Cell-type-specific MMP and TIMP expression. The specific cell types expressing protease and inhibitor mRNA within the inflamed CNS at 6 days p.i. were identified by flow cytometry. The $CD45^-$ population was separated into an astrocyte-enriched population and oligodendroglia. Microglia were separated on the basis of their $CD45^{low}$ phenotype (8, 20, 27). Specific cell surface markers were used to separate neutrophils, macrophages, NK cells, $CD8^+$, and $CD4^+$ T cells within the $CD45^{hi}$-infiltrating cell population (Fig. 1B). Analysis of mRNA expression within the isolated populations demonstrated that MMP-3 mRNA expression was highest within the astrocyte-enriched population (Fig. 5A), consistent with the predominant expression within the $CD45^-$ population (Fig. 1C). Immunohistochemistry supported the idea of expression of MMP-3 protein within cells exhibiting typical astrocyte morphology (Fig. 5B). Finally, colocalization of GFAP and MMP-3 confirmed the identity of astrocytes as the cell type expressing MMP-3 protein in the coronavirus-infected CNS parenchyma (Fig. 5C). These data confirm the transcriptional mRNA upregulation at the protein level and demonstrate that MMP-3 expression is limited to astrocytes during coronavirus-induced encephalitis.

In contrast to the astrocyte-restricted expression of MMP-3, MMP-12 mRNA was detected in multiple CNS resident and inflammatory cell types isolated from the inflamed CNS (Fig. 6). Among CNS resident cells, oligodendroglia expressed the highest levels of MMP-12 mRNA, although increased mRNA levels were also detected in the astrocyte-enriched population as well as microglia. Within the inflammatory cell populations, the highest levels of MMP-12 mRNA expression were detected in $CD4^+$ T cells, neutrophils, and macrophages (Fig. 6). Consistent with the broad distribution of MMP-12 mRNA, no specific cell population expressing MMP-12 within the inflamed CNS could be identified by immunohistochemistry due to diffuse protein expression in both the CNS gray and white matter (data not shown). These data indicate that in contrast to the astrocyte-restricted expression of MMP-3, MMP-12 is expressed by a variety of cell types during coronavirus-induced encephalitis.

TIMP-1 expression prevailed within the $CD45^{hi}$ population derived from the infected CNS (Fig. 1C) but increased in the $CD45^-$ population following immunosuppression (Fig. 3). Fractionation of CNS-derived cell populations at day 6 p.i.

TABLE 2. Kinetics of brain cytokine-chemokine mRNA expression in the CNS following JHMV infection

Day p.i.	mRNA expression relative to ubiquitin							
	IL-1α	IL-1β	IL-6	IFN-β	TNF-α	IFN-γ	CCL-2	CCL-5
Naïve	37	278	ND[a]	ND	7	ND	17	41
2	71	137	6.1	1	48	6	87	107
4	109	379	15	36	494	51	417	317
6	657	636	126	54	236	294	2,637	1,667
8	417	539	67	25	285	483	3,549	9,582
10	141	191	20	3	88	225	861	7,291
14	42	184	5	ND	57	135	680	3,246

[a] ND, not detectable.

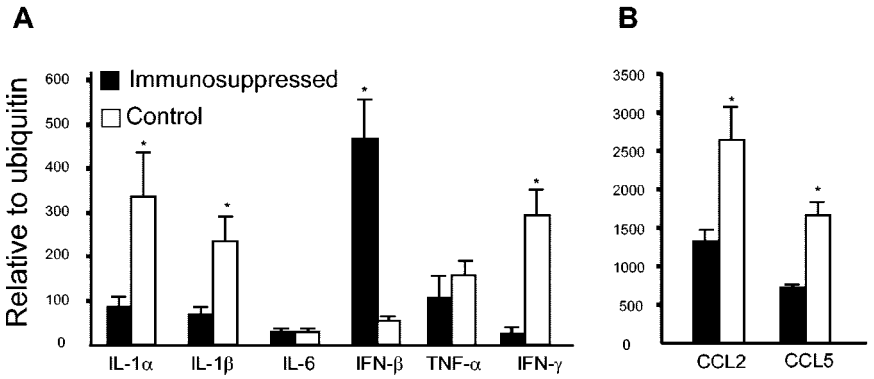

FIG. 4. Expression of cytokines and chemokines in the brains of infected untreated and immunosuppressed infected mice. Relative levels of mRNA expression of cytokine (A) and chemokine (B) mRNA in brains of untreated control and immunosuppressed infected mice at day 6 p.i. are shown. Data represent the average results obtained for three to five mice per group. Error bars represent SD. *, $P < 0.05$.

showed that $CD4^+$ T cells expressed the highest level of TIMP-1 mRNA (Fig. 7). NK cells and $CD8^+$ T cells also expressed TIMP-1 mRNA; however, the level was only ~30% of the level detected in $CD4^+$ T cells. Only minimal TIMP-1 mRNA was detected within any CNS resident cell population or within infiltrating macrophages (Fig. 7), contrasting with TIMP-1 expression by astrocytes during EAE (19, 21). The vast majority of cells expressing TIMP-1 protein in the encephalitic CNS localized to the perivascular and subarachnoid spaces (Fig. 6B), consistent with the localization of $CD4^+$ T cells to

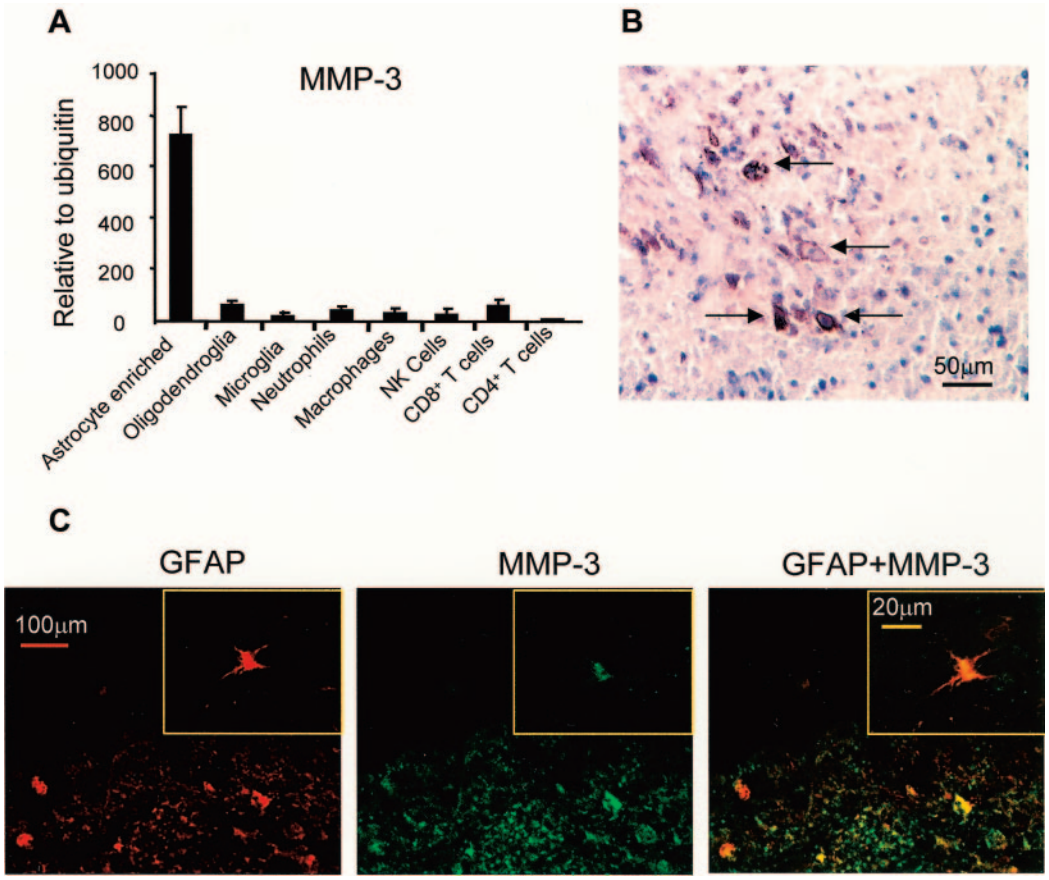

FIG. 5. Astrocyte expression of MMP-3 during virus-induced encephalitis. (A) Expression of MMP-3 mRNA in CNS resident and inflammatory cells isolated by FACS at day 6 p.i. Samples were pooled from four to seven mice/experiment. mRNA levels determined by real-time PCR are presented relative to ubiquitin mRNA expression levels. Data represent the average results of three experiments. (B) MMP-3 protein expression in the infected CNS. Arrows indicate cells giving positive results. (C) MMP-3 colocalizes with GFAP by confocal microscopy. MMP-3-expressing cells were detected with a tetramethyl rhodamine isothiocyanate conjugate (red). GFAP positive cells were detected with an FITC conjugate (green). Cells coexpressing MMP-3 and GFAP are yellow.

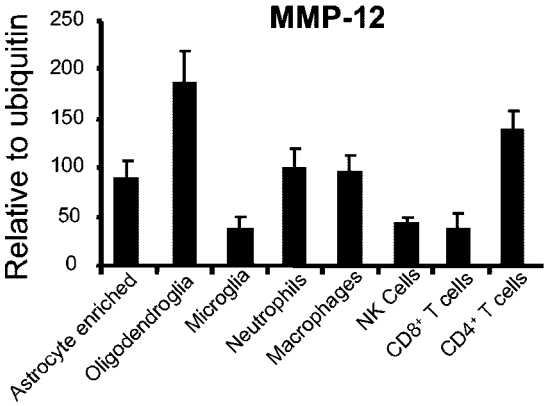

FIG. 6. MMP-12 mRNA expression in CNS-derived cells. CNS resident and inflammatory cells were isolated by FACS from pools of four to seven infected mice/experiment at day 6 p.i. Data represent the average results of three experiments. MMP-12 mRNA levels were determined by real-time PCR and are presented relative to ubiquitin mRNA expression levels.

these regions during acute coronavirus-induced encephalitis (27) (Fig. 7B). By contrast, $CD8^+$ T cells localized predominantly within the CNS parenchyma during coronavirus infection (3, 17) (Fig. 7B). Coexpression of TIMP-1 and CD4 by cells localized to the perivascular areas and subarachnoid spaces confirms the restricted TIMP-1 protein expression by inflammatory $CD4^+$ T cells recruited into the CNS during coronavirus-induced encephalitis (Fig. 7C). Only rare TIMP-1-expressing cells were detected in the CNS parenchyma (Fig. 7C). Although mRNA analysis suggested low levels of TIMP-1 expression by $CD8^+$ T cells, NK cells, and cells within the $CD45^-$ population (Fig. 7A), no colocalization of TIMP-1 protein expression and CD8 or GFAP was detected either in the perivascular areas or within the CNS parenchyma (data not shown). Whether this reflects the insensitivity of the method used or the absence of TIMP-1 expression is unknown; however, the data clearly demonstrate abundant expression of TIMP-1 by the $CD4^+$ T cells localized to the CNS perivascular regions.

These data demonstrate that the majority of TIMP-1 mRNA and all detectable TIMP-1 protein are expressed by $CD4^+$ T cells. To determine whether the $CD4^+$ T cells in the peripheral immune compartment expressed MMP and TIMP mRNA and whether expression was regulated by activation, MMP and TIMP mRNAs from $CD4^+$ T cells purified from the spleens of naïve mice before and following in vitro stimulation were compared. MMP-3 mRNA was expressed at barely detectable levels by $CD4^+$ T cells isolated from naïve mice (Fig. 8), in similarity to the results seen with $CD4^+$ T cells isolated from the inflamed CNS (Fig. 5). By contrast, mRNAs encoding MMP-2, MMP-9, MMP-12, MMP-14, TIMP-1, TIMP-2, and TIMP-3 were all readily detected in $CD4^+$ T cells from naïve mice (Fig. 8). However, whereas the levels of the majority of mRNA species examined decreased following activation, the levels of mRNA encoding TIMP-1 increased (Fig. 8). These data suggest a correlation between $CD4^+$ T-cell activation and TIMP-1 expression and the inability of activated $CD4^+$ T cells to access the CNS parenchyma.

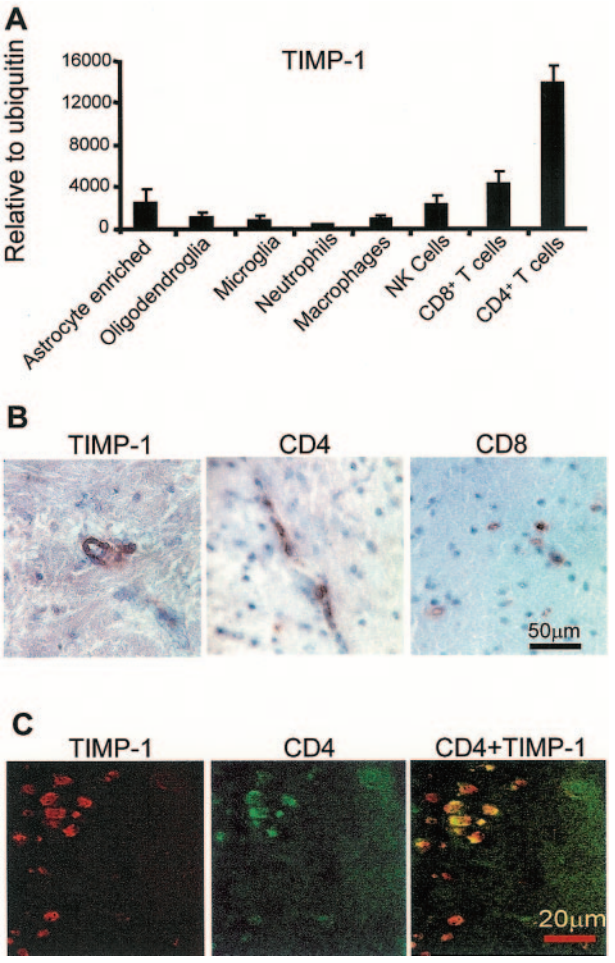

FIG. 7. TIMP-1 expression by $CD4^+$ T cells. (A) CNS resident and inflammatory cells isolated by FACS were pooled from four to seven infected mice/experiment at day 6 p.i. Data represent the average results of three experiments. TIMP-1 mRNA levels were determined by real-time PCR are presented relative to ubiquitin mRNA expression levels. (B) Distribution of TIMP-1, $CD4^+$ T, and $CD8^+$ T cells in brains of infected mice. (C) Colocalization of TIMP-1 and CD4. TIMP-1-expressing cells were detected with a Cy3 conjugate (red). $CD4^+$ T cells were detected with an FITC conjugate (green). Cells coexpressing TIMP-1 and CD4 are yellow.

DISCUSSION

Inflammatory cells are recruited into target tissues in response to signals, including cytokine and chemokine gradients (25). Chemokines and other innate immune effector molecules increase adhesion molecule expression on endothelial cells, facilitating the prerequisite transient interactions between inflammatory cells and endothelial surfaces required for tissue entry (12, 23, 25). Endothelial cells in most tissues constitutively express high levels of adhesion molecules, allowing T cells to sample the tissue environment, even in the absence of infection (12). By contrast, CNS endothelia are characterized by low constitutive adhesion molecule expression and tight cell-cell junctions that contribute to the selective permeability of the BBB (2, 12, 23), thereby restricting access of lymphocytes to the CNS. MMPs not only facilitate access of T cells into the CNS via disruption of the BBB but also potentially

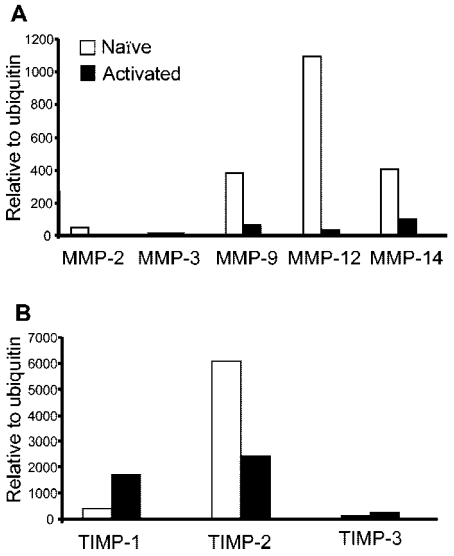

FIG. 8. MMP and TIMP expression in naïve versus activated $CD4^+$ T cells. $CD4^+$ T cells were purified by positive selection from BALB/c mice and activated with PMA and ionomycin for 12 h. MMP and TIMP mRNA levels in untreated and activated $CD4^+$ T cells were determined by real-time PCR and are presented relative to ubiquitin mRNA expression levels.

contribute to the inflammatory response via disruption of the CNS parenchymal ECM. Indeed, MMP activity in the parenchyma has been implicated in both neuronal death and myelin loss (11, 20, 32) suggesting a direct role in CNS pathology (10). Among the diverse MMP family members, MMP-9 appears most critical to CNS inflammation. Consistent with its critical role in BBB disruption (34) it is found in MS lesions, which are associated with both the entry of encephalitogenic $CD4^+$ T cells during EAE (11, 19, 20, 21, 32) and a variety of viral and bacterial CNS infections (6, 14, 15, 34).

In contrast to the apparent universal involvement of MMP-9, other MMP members are associated with different etiologies of CNS inflammation. For example, MMP-9, MMP-2, and MMP-7 are associated with HIV dementia (6), while MMP-8 is associated with bacterial meningitis (16). Only MMP-3 and MMP-12 mRNAs, in conjunction with neutrophil-derived preformed MMP-9 protein, are expressed during coronavirus-induced encephalitis (33, 34). Increased MMP-12 expression by a variety of cell types is consistent with increased expression during EAE (19, 21) and its association with active MS lesions (11, 20, 30, 32). Nevertheless, induction of this limited repertoire of MMPs during infection of the murine CNS is strikingly different from the diversity of MMPs induced during $CD4^+$ T-cell-mediated CNS autoimmunity, which includes MMP-2, -3, -8, -9, -10, -12, -13, and -14 (11, 19, 21, 32). Possible explanations for this differential expression pattern within a single target organ include the diverse inflammatory cells recruited or the nature of the insult itself. During coronavirus infection, both innate and adaptive cellular components traffic into the CNS (3, 17, 34), resulting in an acute encephalomyelitis accompanied by myelin loss. $CD8^+$ T cells are the major effectors of virus clearance (3, 17), while both $CD4^+$ and $CD8^+$ T cells contribute to myelin loss (3, 24). On the other hand, although $CD4^+$ T cells are required for induction of EAE, prominent $CD4^+$ T-cell recruitment into the CNS is accompanied by a variety of other cells, including macrophages (28). These observations suggest that the cytokine or chemokine milieu induced, rather than the infiltrating cells themselves or tissue damage, i.e., myelin destruction common to both EAE and the later stages of coronavirus-induced encephalomyelitis, may play regulatory roles in specific MMP induction. Coronavirus replication induces the expression of a variety of chemokines and cytokines prior to T-cell infiltration (10, 22, 26, 33). Similar kinetics of increases in MMP-3 and MMP-12 mRNA versus IL-1α, IL-1β, and IFN-β mRNA levels supported a correlation of CNS resident MMP mRNA induction and cytokines associated with innate, rather than adaptive, immunity.

Furthermore, immunosuppression did not inhibit MMP mRNA induction but rather specifically increased levels of MMP-3, MMP-12, and TIMP-1 mRNA. This suggests that virus replication itself is sufficient to induce the expression of a subset of MMPs in the absence of inflammation. Enhanced proteolytic activity in this case may be balanced by increased TIMP-1 expression. Similar to coronavirus infection of immunosuppressed hosts, TIMP-1 is expressed by CNS resident cells during EAE (19, 21). The notion that TIMP-1 expression may reflect an attempt of the target tissue to limit CNS damage potentially induced by MMPs is supported by a correlation between deceased TIMP-1 and increased MMP levels during MS exacerbations and a poor prognosis (11, 20, 31, 32). A critical role of TIMPs in regulating progression of CNS autoimmune disease is also clearly evident by the amelioration of EAE following treatment with MMP inhibitors (4, 11, 20, 32).

It is difficult to discern whether increased MMP levels in immunosuppressed mice are directly associated with increased virus replication and concomitant reduced induction of IL-1α and IL-1β, increased IFN-β mRNA levels, or the lack of CNS inflammatory cells. Comparison of MMP and cytokine induction in the inflamed and immunosuppressed CNS implicated IFN-β as a possible regulatory cytokine for MMP induction during virus-induced encephalitis. However, this concept contrasts with the role of IFN-β as a useful therapeutic agent in some MS patients and with its inhibition of MMP secretion by T cells in vitro (15). The putative role of IFN-β in inhibiting $CD4^+$ T-cell-mediated autoimmune disease may reflect differences in MMP regulation during autoimmune disease and virus-mediated induction of IFN-β. Alternatively, virus replication may induce MMP-3, MMP-12, and TIMP-1 mRNA and repress activation of other MMP and TIMP mRNAs via a complex of cytokine and/or chemokine synergistic interactions. For example, IL-1β and TNF-α act synergistically to increase TIMP-1 mRNA while repressing TIMP-3 expression in brain microvascular cells (5). No changes in the restricted expression pattern of MMP-3, MMP-12, and TIMP-1 or in TNF-α and IL-6 mRNA levels in the infected CNS of immunocompromised mice compared to the results seen with control mice support the notion of virus-mediated regulation of MMP expression.

TIMP-1 is expressed by astrocytes during EAE (19, 21). TIMP-1 is also present within MS lesions (11, 20, 32) and has been detected in cerebrospinal fluid of MS patients during active disease and in patients with viral meningitis (6, 11, 14,

15, 20, 31, 32). By contrast, the majority of cells within the CNS expressing TIMP-1 during coronavirus-induced encephalitis are $CD4^+$ T cells localized within the perivascular and subarachnoid spaces. The majority of $CD8^+$ T cells, by contrast, are found within the CNS parenchyma, and only very rare TIMP-1-expressing cells were detected in the parenchyma. These data suggest that TIMP-1 expression by $CD4^+$ T cells is inversely correlated with the ability to migrate into the CNS parenchyma. This concept is consistent with increased TIMP-1 expression in human peripheral $CD4^+$ T cells versus $CD8^+$ T cells (13), increased expression of TIMP-1 by activated peripheral murine $CD4^+$ T cells, and the inability of B cells, which express low levels of TIMP-1, to traverse the BBB (1). Neutrophil-derived MMP-9 is critical for disruption of BBB integrity, thereby allowing inflammatory cells to enter the perivascular and subarachnoid spaces (11, 20, 31, 32, 34). The present data further show increased MMP-12 mRNA levels in $CD4^+$ cells compared to $CD8^+$ T cells, suggesting the possibility that expression of additional MMPs may be required for T cells to access the ECM-rich parenchyma. However, the differential expression of TIMP-1 by $CD4^+$ T cells implies an additional regulatory role for TIMPs in preventing or delaying access to the CNS parenchyma. By contrast, $CD8^+$ T cells, the primary effectors of CNS viral vclearance (2, 17), do not express TIMP-1 and traffic into the parenchyma in search of virus-infected cells (2, 27).

The analysis of MMP and TIMP mRNA expression by individual cell populations isolated from the inflamed CNS, coupled with immunohistochemistry, provides insight into the potential mechanisms contributing to the differential trafficking of T cells within the CNS during coronavirus-induced encephalitis (17, 27). These data suggest that the diversity of MMP and inhibitor expression plays a role in shaping CNS inflammatory processes and further suggest a direct correlation with the differential ability of inflammatory cells to access the CNS parenchyma during virus-induced encephalitis. Expression of TIMP-1 by $CD4^+$ T cells provides a novel insight into differential T-cell trafficking into virus-infected tissue and emphasizes the importance of T-cell localization in controlling viral pathogenesis of the CNS.

ACKNOWLEDGMENTS

This work was supported by Public Health Service grants NS18146 and NS40667 from the National Institutes of Health.

REFERENCES

1. **Alter, A., M. Duddy, S. Herbert, K. Biernacki, A. Prtat, J. Antel, V. W. Yong, R. K. Nuttall, C. J. Pennington, D. R. Edwards, and A. Bar-Or.** 2003. Determinants of human B cell migration across brain endothelial cells. J. Immunol. **170:**4497–4505.
2. **Bart, J., H. J. Groen, N. K. Hendrikse, W.T. van der Graaf, W. Vaalburg, and E. G. de Vries.** 2000. The blood-brain barrier and oncology: new insights into function and modulation. Cancer Treat. Rev. **26:**449–462.
3. **Bergmann, C., B. Parra, D. R. Hinton, C. Ramakrishna. M. Morrison, and S. A. Stohlman.** 2003. Perforin mediated effector function within the CNS requires IFN-g mediated MHC upregulation. J. Immunol. **170:**3204–3213.
4. **Brosnan, C. F., W. Cammer, W. T. Norton, and R. Bloom.** 1980. Proteinase inhibitors suppress the development of experimental allergic encephalomyelitis. Nature **285:**235–237.
5. **Bugnu, M., B. Witek, J. Bereta, M. Bereta, D. R. Edwards, and T. Kordula.** 1999. Reprogramming of TIMP-1 and TIMP-3 expression profiles in brain microvascular endothelial cells and astrocytes in response to proinflammatory cytokines. FEBS Lett. **448:**9–14.
6. **Conant, K., J. C. McAuthur, D. E. Griffin, L. Sjulson, L. M. Whal, and D. N. Irani.** 1999. Cerebrospinal fluid levels of MMP-2, 7 and 9 are elevated in association with human immunodeficiency virus dementia. Ann. Neurol. **46:**391–398.
7. **Fleming, J. O., M. D. Trousdale, F.A. el-Zaatari, S. A. Stohlman, and L. P. Weiner.** 1986. Pathogenicity of antigenic variants of murine coronavirus JHM selected with monoclonal antibodies. J. Virol. **58:**869–875.
8. **Ford, A. L., A. L. Goodsall, W. F. Hickey, and J. D. Sedgwick.** 1995. Normal adult ramified microglia separated from other central nervous system macrophages by flow cytometric sorting. J. Immunol. **154:**4309–4321.
9. **Fuss, B., B. Mallon, T. Phan, C. Ohlemeyer, F. Kirchhoff, A. Nishiyama, and W. B. Macklin.** 2000. Purification and analysis of in vivo-differentiated oligodendrocytes expressing the green fluorescent protein. Dev. Biol. **218:**259–274.
10. **Glass, W. G., B. J. Chen, M. T. Liu, and T. E. Lane.** 2002. Mouse hepatitis virus infection of the central nervous system: chemokine-mediated regulation of host defense and disease. Viral Immunol. **15:**261–272.
11. **Hartung, H. P., and B. C. Kieseier.** 2000. The role of matrix metalloproteinases in autoimmune damage to the central and peripheral nervous system. J. Neuroimmunol. **107:**140–147.
12. **Hickey, W. F.** 2001. Basic principles of immunological surveillance of the normal central nervous system. Glia **36:**118–124.
13. **Johnatty, R. N., D. D. Taub, S. P. Reeder, S. M. Turcoviki-Corrales, D. W. Cottam, T. J. Stephenson, and R. C. Rees.** 1997. Cytokine and chemokine regulation of proMMP-9 and TIMP-1 production by human peripheral blood lymphocytes. J. Immunol. **158:**2327–2333.
14. **Kolb, S. A., F. Lahrtz, R. Paul, D. Leppert, D. Nadal, H. W. Pfister, and A. Fontana.** 1998. Matrix metalloproteinases and tissue inhibitors of metalloproteinases in viral meningitis: upregulation of MMP-9 and TIMP-1 in cerebrospinal fluid. J. Neuroimmunol. **84:**143–150.
15. **Leppert, D., S. L. Leib, C. Grygar, K. M. Miller, U. B. Schaad, and G. A. Hollander.** 2000. Matrix metalloproteinase (MMP)-8 and MMP-9 in cerebrospinal fluid during bacterial meningitis: association with blood-brain barrier damage and neurological sequelae. Clinical Infect. Dis. **31:**80–84.
16. **Leppert, D., E. Waubant, W. R. Burk, J. R. Oksenberg, and S. L. Hauser.** 1996. Interferon Beta-1b inhibits gelatinase secretion and in vitro migration of human T cells: a possible mechanism for treatment efficacy in multiple sclerosis. Ann. Neurol. **40:**846–852.
17. **Marten, N. W., S. A. Stohlman, and C. C. Bergmann.** 2001. MHV infection of the CNS: mechanisms of immune-mediated control. Viral Immunol. **14:**1–18.
18. **Nagase, H., and J. G. Woessner.** 1999. Matrix metalloproteinases. J. Biol. Chem. **274:**21491–21494.
19. **Nygardas, P. T., and A. E. Hinkkanen.** 2002. Up-regulation of MMP-8 and MMP-9 activity in the BALB/c mouse spinal cord correlates with the severity of experimental autoimmune encephalitis. Clin. Exp. Immunol. **128:**245–254.
20. **Ozenci, V., L. Rinaldi, N. Teleshova, D. Matusevicius, P. Kivisakk, M. Kouwenhoven, and H. Link.** 1999. Metalloproteinases and their tissue inhibitors in multiple sclerosis. J. Autoimmun. **12:**297–303.
21. **Pagenstecher, A., A. K. Stalder, C. L. Kincaid, S. D. Shapiro, and I. L. Campbell.** 1998. Differential expression of matrix metalloproteinase and tissue inhibitor of matrix metalloproteinase genes in the mouse central nervous system in normal and inflammatory states. Am. J. Pathol. **152:**729–741.
22. **Parra, B., D. R. Hinton, M. T. Lin, D. J. Cua, and S. A. Stohlman.** 1997. Kinetics of cytokine mRNA expression in the central nervous system following lethal and nonlethal coronavirus-induced acute encephalomyelitis. Virology **233:**260–270.
23. **Perry, V. H., D. C. Anthony, S. J. Bolton, and H. C. Brown.** 1997. The blood-brain barrier and the inflammatory response. Mol. Med. Today **3:**335–341.
24. **Pewe, L., J. Haring, and S. Perlman.** 2002. CD4 T-cell-mediated demyelination is increased in the absence of gamma interferon in mice infected with mouse hepatitis virus. J. Virol. **76:**7329–7333.
25. **Ransohoff, R. M., P. Kivisakk, and G. Kidd.** 2003. Three or more routes for leukocyte migration into the central nervous system. Nat. Rev. Immunol. **3:**569–581.
26. **Rempel, J. D., S. J. Murray, J. Meisner, and M. J. Buchmeier.** 2004. Differential regulation of innate and adaptive immune responses in viral encephalitis. Virology **318:**381–392.
27. **Stohlman, S. A., C. C. Bergmann, M. T. Lin, D. J. Cua, and D. R. Hinton.** 1998. CTL effector function within the central nervous system requires $CD4^+$ T cells. J. Immunol. **160:**2896–2904.
28. **Tran, E. H., E. Prince, and T. Owens.** 2000. IFN-g shapes immune invasion of the central nervous system via regulation of chemokines. J. Immunol. **164:**2759–2768.
29. **Visse, R., and H. Nagase.** 2003. Matrix metalloproteinases and tissue inhibitors of metalloproteinases: structure, function and biochemistry. Circ. Res. **92:**827–839.
30. **Vos, C. M. P., E. S. van Haastert, C.J.A. de Groot, P. van der Valk, and P. H. E. de Vries.** 2003. Matrix metalloproteinase-12 is expressed in phagocytic macrophages in active multiple sclerosis lesions. J. Neuroimmunol. **138:**106–114.
31. **Waubant, E., D. E. Goodkin, L. Gee, P. Bacchetti, R. Sloan, T. Stewart, P. B.**

Andersson, G. Stabler, and K. Miller. 1999. Serum MMP-9 and TIMP-1 levels are related to MRI activity in relapsing multiple sclerosis. Neurology **53:**1397–1401.
32. **Yong, V. W., C. Power, P. Forsyth, and D. R. Edwards.** 2001. Metalloproteinases in biology and pathology of the nervous system. Nat. Rev. Neurosci. **2:**502–511.
33. **Zhou, J., S. A. Stohlman, R. Atkinson, D. R. Hinton, and N. W. Marten.** 2002. Matrix metalloproteinase expression correlates with virulence following neurotropic mouse hepatitis virus infection. J. Virol. **76:**7374–7384.
34. **Zhou, J., S. A. Stohlman, D. R. Hinton, and N. W. Marten.** 2003. Neutrophils promote mononuclear cell infiltration during viral-induced encephalitis. J. Immunol. **170:**3331–3336.